HARMONIC RETRIEVAL FOR NON-CIRCULAR COHERENT SIGNALS VIA DOUBLE DECOUPLED ATOMIC NORM MINIMIZATION

Yu Zhang[⋆] *Yue Wang*[†] *Zhipeng Cai*[†] *Gong Zhang*[‡]

[⋆] School of EIE, Nanjing University of Information Science and Technology, Nanjing, China
[†] Department of CS, Georgia State University, Atlanta, GA, USA
[‡] College of EIE, Nanjing University of Aeronautics and Astronautics, Nanjing, China

ABSTRACT

This paper studies super-resolution harmonic retrieval for strictly non-circular coherent signals. We develop gridless sparse representations of both their covariance and pseudo-covariance matrices over a common matrix-form atom set. This enables the decoupled atomic norm minimization (D-ANM) technique to exploit the sparsity of the covariance and pseudo-covariance matrices jointly. Further, by effectively utilizing the inherent mutual coupling characteristics between the covariance and pseudo-covariance matrices, additional constraints are properly imposed to reflect and enforce desired structure information represented by such matrices and their augmented matrix. It leads to a novel structure-based sparse optimization method, called double decoupled atomic norm minimization (DD-ANM). In addition, performance analysis is provided for the proposed DD-ANM method in practical settings. Simulation results reveal that the proposed DD-ANM outperforms the benchmark methods in terms of lower estimation errors.

***Index Terms*—** harmonic retrieval, non-circularity, coherent signals, double decoupled atomic norm minimization, covariance.

1. INTRODUCTION

Harmonic retrieval of non-circular (NC) coherent signals with multiple measurement vectors (MMV) has attracted attention in recent years. In fact, many modulated signals used in communication and radar systems are NC in nature [1]. Meanwhile, coherency of source signals widely exists due to multipath propagation in practice [2]. Conventional harmonic retrieval methods have been developed for processing and analyzing NC coherent signals [3–6]. While these methods successfully handle coherent source signals and enjoy enhanced accuracy thanks to the enlarged manifold in NC scenarios, they can only work with uniform linear arrays but fail to perform well under the subsampling or compression scenarios.

To overcome this problem, compressed sensing (CS) based algorithms are developed to utilize the sparsity of sources [7,8]. However, these solutions based on on-grid assumption suffer from limited estimation accuracy due to basis mismatch. Although a covariance matrix gridless sparse representation (CMGSR) approach has been proposed for coherent signals via a gridless technique called as atomic norm minimization (ANM) [9], it only deals with the covariance matrix. Recently, we develop a low-rank Toeplitz-Hankel covariance reconstruction method based on another type of gridless technique termed as low-rank structured covariance reconstruction for harmonic retrieval of NC signals [10]. It exploits the structural information of both the covariance and pseudo-covariance matrices at the same time. Unfortunately, such structural information no longer holds under coherent scenarios. To the best of our knowledge, there still lacks gridless-type method for NC coherent signals by jointly capturing the sparsity of both covariance and pseudo-covariance for high estimation accuracy with high sample efficiency.

To fill this gap, this work aims at efficient ANM-based method for harmonic retrieval of NC coherent signals, by exploiting the sparsity of covariance and pseudo-covariance matrices jointly and also by utilizing the mutual coupling characteristics between them. To this end, we first develop gridless sparse representations of both the covariance and pseudo-covariance matrices over a common matrix-form atom set, which permits an effectively joint utilization of the sparsity of such two matrices via the decoupled ANM (D-ANM) technique. Then, by utilizing the inherent mutual coupling characteristics between the covariance and pseudo-covariance matrices, we introduce additional constraints to properly reflect and enforce some desired structure information represented by such matrices and their augmented matrix. This gives rise to a novel structure-based sparse optimization solution, named double D-ANM (DD-ANM) for harmonic retrieval of NC coherent signals. Theoretical analysis and simulation results verify the advantage of the proposed DD-ANM.

Notations: a, $\boldsymbol{a}$, $\boldsymbol{A}$ and $\mathcal{A}$ denote a scalar, a vector, a matrix and a set, respectively. $(\cdot)^T$, $(\cdot)^*$, and $(\cdot)^H$ are the transpose, conjugate, and conjugate transpose of a vector or matrix, respectively. $\text{diag}(\boldsymbol{a})$ generates a diagonal matrix with the diagonal elements constructed from $\boldsymbol{a}$ and $\text{blkdiag}([\boldsymbol{A}_1, \boldsymbol{A}_2])$ returns the block diagonal matrix created by aligning $\boldsymbol{A}_1$ and $\boldsymbol{A}_2$ along the diagonal direction. $\text{vec}(\cdot)$ stacks all the columns of a matrix into a vector. $\boldsymbol{I}_\Omega$ is generated from an identity matrix by selecting its rows with indices Ω, and $\boldsymbol{0}_a$ is an a-size zeros matrix. $\text{T}(\boldsymbol{u})$ represents a hermitian Toeplitz matrix with the first column being $\boldsymbol{u}$. $\text{Tr}(\boldsymbol{A})$ denotes the trace of $\boldsymbol{A}$. For a scalar a, $|a|$ denotes its modulus and for a set $\mathcal{A}$, $|\mathcal{A}|$ is the cardinal number of $\mathcal{A}$. $\|\cdot\|_2$ and $\|\cdot\|_F$ denote the Euclidean and Frobenius norm, respectively. $\mathbb{E}\{\cdot\}$ denotes expectation.

2. SIGNAL MODEL AND PROBLEM FORMULATION

Consider the problem of harmonic retrieval from a strictly NC coherent signal. The NC signal of interest $\boldsymbol{x}(t) \in \mathbb{C}^M$ is a linear mixture of K frequency components in the form of

$$\begin{aligned}\boldsymbol{x}(t) &= \sum_{i=1}^{K} s_i(t)\boldsymbol{a}(f_i) = \sum_{i=1}^{K} s_i'(t)e^{j\phi_i}\boldsymbol{a}(f_i), \\ &= \boldsymbol{A}(\boldsymbol{f})\boldsymbol{s}(t) = \boldsymbol{A}\boldsymbol{\Phi}\boldsymbol{s}'(t) \quad t = 1, \ldots, L,\end{aligned} \tag{1}$$

This work was supported in part by the NSFC grants #62271255, #61871218, and #61801211, the US NSF grants #2136202 and #2231209, and the key laboratory of Radar imaging and microwave photonics (NUAA), ministry of education, grants #NJ2023008.

where $s_i(t) = s'_i(t)e^{j\phi_i}$ is the complex exponential of the i-th source signal at the t-th snapshot with real-valued amplitude $s'_i(t)$, $\boldsymbol{f} = [f_1, \ldots, f_K]^T$ with $f_i \in (-\frac{1}{2}, \frac{1}{2}]$ consists of the digital frequencies of $\boldsymbol{x}(t)$, and L is the number of snapshots. By strict noncircularity, the phase terms ϕ_i of source signals are unchanged for all snapshots t, unlike circular signals. The manifold matrix $\boldsymbol{A} = \boldsymbol{A}(\boldsymbol{f}) = [\boldsymbol{a}(f_1), \ldots, \boldsymbol{a}(f_K)]$ is made of Vandermonde-structured steering vectors $\boldsymbol{a}(f_i)$ of size M:

$$\boldsymbol{a}(f_i) = [1, \exp(j2\pi f_i), \ldots, \exp(j2\pi(M-1)f_i)]^T. \quad (2)$$

Further, $\boldsymbol{s}(t) = \boldsymbol{\Phi}\boldsymbol{s}'(t) = [s_1(t), \ldots, s_K(t)]^T$ with $\boldsymbol{s}'(t) = [s'_1(t), \ldots, s'_K(t)]^T$ and $\boldsymbol{\Phi}$=diag($\boldsymbol{\phi}$)=diag($[e^{j\phi_1}, \ldots, e^{j\phi_K}]^T$) being a diagonal matrix.

In many applications, $\boldsymbol{x}(t)$ is not observed directly, but through subsampling or linear compression via a measurement matrix $\boldsymbol{J} \in \mathbb{C}^{N\times M}$ with $N \leq M$. Inflicted by an additive noise $\boldsymbol{n}(t)$, the single measurement vector data $\boldsymbol{y}(t) \in \mathbb{C}^N$ is given by

$$\boldsymbol{y}(t) = \boldsymbol{J}\boldsymbol{x}(t) + \boldsymbol{n}(t) = \boldsymbol{J}\boldsymbol{A}\boldsymbol{\Phi}\boldsymbol{s}'(t) + \boldsymbol{n}(t). \quad (3)$$

Then, the covariance and the pseudo-covariance of $\boldsymbol{y}(t)$ can be respectively expressed as

$$\begin{aligned} \boldsymbol{R}_y &= \mathbb{E}\{\boldsymbol{y}(t)\boldsymbol{y}^H(t)\} = \boldsymbol{J}\boldsymbol{R}_x\boldsymbol{J}^H + \boldsymbol{R}_n, \\ \boldsymbol{C}_y &= \mathbb{E}\{\boldsymbol{y}(t)\boldsymbol{y}^T(t)\} = \boldsymbol{J}\boldsymbol{C}_x\boldsymbol{J}^T, \end{aligned} \quad (4)$$

where $\boldsymbol{R}_x$ is the covariance matrix of $\boldsymbol{x}(t)$ given by

$$\boldsymbol{R}_x = \mathbb{E}\{\boldsymbol{x}(t)\boldsymbol{x}^H(t)\} = \boldsymbol{A}\boldsymbol{R}_s\boldsymbol{A}^H = \boldsymbol{A}\boldsymbol{\Phi}\boldsymbol{R}_{s'}\boldsymbol{\Phi}^*\boldsymbol{A}^H, \quad (5)$$

where $\boldsymbol{R}_s = \mathbb{E}\{\boldsymbol{s}(t)\boldsymbol{s}^H(t)\}$, $\boldsymbol{R}_{s'} = \mathbb{E}\{\boldsymbol{s}'(t)\boldsymbol{s}'^T(t)\}$ and $\boldsymbol{R}_s = \boldsymbol{\Phi}\boldsymbol{R}_{s'}\boldsymbol{\Phi}^*$. Note that herein $\boldsymbol{R}_{s'}$ is a non-diagonal matrix for correlated/coherent sources, and so is $\boldsymbol{R}_s$, which is a key difference from uncorrelated sources. The pseudo-covariance matrix $\boldsymbol{C}_x$ of $\boldsymbol{x}(t)$ is formed as

$$\boldsymbol{C}_x = \mathbb{E}\{\boldsymbol{x}(t)\boldsymbol{x}^T(t)\} = \boldsymbol{A}\boldsymbol{C}_s\boldsymbol{A}^T = \boldsymbol{A}\boldsymbol{\Phi}\boldsymbol{R}_{s'}\boldsymbol{\Phi}\boldsymbol{A}^T, \quad (6)$$

where $\boldsymbol{C}_s = \mathbb{E}\{\boldsymbol{s}(t)\boldsymbol{s}^T(t)\} = \boldsymbol{\Phi}\boldsymbol{R}_{s'}\boldsymbol{\Phi}$. Denote $r'_{i,j}$, $r_{i,j}$ and $c_{i,j}$ as the i-th row and the j-th column element in $\boldsymbol{R}'_s$, $\boldsymbol{R}_s$ and $\boldsymbol{C}_s$, respectively, then we have

$$\begin{cases} r'_{i,j} = 0 & s'_i(t), s'_j(t) \text{ uncorrelated} \\ r'_{i,j} \neq 0 & s'_i(t), s'_j(t) \text{ correlated,} \end{cases} \quad (7)$$

$$r_{i,j} = r'_{i,j}e^{j(\phi_i - \phi_j)}, \quad c_{i,j} = r'_{i,j}e^{j(\phi_i + \phi_j)}, \quad (8)$$

and

$$|r_{i,j}| = |c_{i,j}| = |r'_{i,j}|. \quad (9)$$

In practice, $\boldsymbol{R}_y$ and $\boldsymbol{C}_y$ are approximated from finite snapshots as $\hat{\boldsymbol{R}}_y = \frac{1}{L}\sum_{t=1}^{L}\boldsymbol{y}(t)\boldsymbol{y}^H(t)$ and $\hat{\boldsymbol{C}}_y = \frac{1}{L}\sum_{t=1}^{L}\boldsymbol{y}(t)\boldsymbol{y}^T(t)$, respectively. Then, the goal of harmonic retrieval of NC coherent signals in this paper is to recover $\{f_i\}_i$ from $\hat{\boldsymbol{R}}_y$ and $\hat{\boldsymbol{C}}_y$ jointly.

When only deal with the covariance matrix $\boldsymbol{R}_y$, note that

$$\boldsymbol{R}_y = \boldsymbol{J}\boldsymbol{A}\boldsymbol{R}_s\boldsymbol{A}^H\boldsymbol{J}^H + \boldsymbol{R}_n = \boldsymbol{J}\boldsymbol{A}\boldsymbol{P}_R + \boldsymbol{R}_n = \boldsymbol{J}\boldsymbol{R}_0 + \boldsymbol{R}_n, \quad (10)$$

where

$$\boldsymbol{R}_0 = \boldsymbol{A}\boldsymbol{P}_R = \sum_{i=1}^{K}\|\boldsymbol{p}_i\|_2\,\boldsymbol{a}(f_i)\frac{\boldsymbol{p}_i}{\|\boldsymbol{p}_i\|_2} \in \mathbb{C}^{M\times N} \quad (11)$$

with $\boldsymbol{P}_R = \boldsymbol{R}_s\boldsymbol{A}^H\boldsymbol{J}^H = [\boldsymbol{p}_1^T, \ldots, \boldsymbol{p}_K^T]^T \in \mathbb{C}^{K\times N}$. Define an atom set as $\mathcal{A} = \left\{\boldsymbol{a}(f)\boldsymbol{b}^H \,\middle|\, \forall f \in (-0.5, 0.5], \|\boldsymbol{b}\|_2 = 1, \boldsymbol{b} \in \mathbb{C}^N\right\}$, the atomic norm of $\boldsymbol{R}_0$ over the atom set $\mathcal{A}$ can be defined to seek the sparsest decomposition of $\boldsymbol{R}_0$ over $\mathcal{A}$. Then, the atomic decomposition as well as the frequencies $\{f_i\}_i$ yield the true structure in (11), through the following covariance matrix based gridless sparse representation (CMGSR) method [9]

$$\min_{\boldsymbol{R}_0} \tau_1 \|\boldsymbol{R}_0\|_{A} + \frac{1}{2}\left\|\hat{\boldsymbol{R}}_y - \boldsymbol{J}\boldsymbol{R}_0\right\|_F^2, \quad (12)$$

where τ_1 is a regularization parameter balancing the fitting error term and the sparse term. For (12), it has an equivalent semi-definite programming (SDP) form [11] and can be effectively solved using off-the-shelf convex solvers, such as CVX [12].

Under NC coherent scenarios, we seek to jointly utilize $\hat{\boldsymbol{R}}_y$ and $\hat{\boldsymbol{C}}_y$ to develop high estimation accuracy method. To this end, note that $\boldsymbol{C}_y = \boldsymbol{J}\boldsymbol{C}_x\boldsymbol{J}^T = \boldsymbol{J}\boldsymbol{A}\boldsymbol{C}_s\boldsymbol{A}^T\boldsymbol{J}^T = \boldsymbol{J}\boldsymbol{A}\boldsymbol{P}_C$ where $\boldsymbol{P}_C = \boldsymbol{C}_s\boldsymbol{A}^T\boldsymbol{J}^T \in \mathbb{C}^{K\times N}$ has the same measurement matrix $\boldsymbol{J}$ and manifold matrix $\boldsymbol{A}$ as $\boldsymbol{R}_y$. Then, an intuitive thought is to combine $\boldsymbol{R}_y$ and $\boldsymbol{C}_y$ together to form a MMV as

$$\begin{aligned} \boldsymbol{E}_y &= [\boldsymbol{R}_y, \boldsymbol{C}_y] = \boldsymbol{J}\boldsymbol{A}[\boldsymbol{P}_R, \boldsymbol{P}_C] + [\boldsymbol{R}_n, \boldsymbol{0}_{N\times N}] \\ &= \boldsymbol{J}\boldsymbol{A}\boldsymbol{P}_E + [\boldsymbol{R}_n, \boldsymbol{0}_{N\times N}] = \boldsymbol{J}\boldsymbol{R}_E + [\boldsymbol{R}_n, \boldsymbol{0}_{N\times N}], \end{aligned} \quad (13)$$

where $\boldsymbol{R}_E = \left[\boldsymbol{R}_x\boldsymbol{J}^H, \boldsymbol{C}_x\boldsymbol{J}^T\right] = \boldsymbol{A}\boldsymbol{P}_E$ with $\boldsymbol{P}_E = [\boldsymbol{P}_R, \boldsymbol{P}_C] \in \mathbb{C}^{K\times N'}$, $N' = 2N$. Similar to $\boldsymbol{R}_0$, $\boldsymbol{R}_E$ can be gridless sparse represented over an atom set and we have the following extended CMGSR (E-CMGSR) method for NC coherent signals

$$\min_{\boldsymbol{R}_E} \tau_2 \|\boldsymbol{R}_E\|_{A'} + \frac{1}{2}\left\|\hat{\boldsymbol{E}}_y - \boldsymbol{J}\boldsymbol{R}_E\right\|_F^2, \quad (14)$$

where τ_2 is similarly defined as τ_1 and $\hat{\boldsymbol{R}}_E = \left[\hat{\boldsymbol{R}}_y, \hat{\boldsymbol{C}}_y\right]$. However, the E-CMGSR method in (14) ignores the mutual coupling characteristics between the covariance and pseudo-covariance matrices. Thus, it only take care of the left side manifold of the covariance and pseudo-covariance matrices. In fact, the right side manifold in $\boldsymbol{P}_E$ also contains useful frequency information. As a result, such ignorance limits its estimation performance.

Next, we develop another effective solution for NC coherent signals, by simultaneously exploiting the sparsity of both the covariance and pseudo-covariance matrices jointly and the mutual coupling characteristics between them.

3. PROPOSED METHOD

This section proposes a super-resolution harmonic retrieval method for NC coherent signals. we first develop gridless sparse representations of both the covariance and pseudo-covariance matrices over a common matrix-form atom set, which permits the D-ANM technique to jointly exploit the sparsity of them. Then, by utilizing the inherent mutual coupling characteristics between them, we introduce additional constraints to properly reflect and enforce some desired structure information represented by such matrices and their augmented matrix, which leads to a structure-based gridless sparse optimization solution for harmonic retrieval of NC coherent signals.

3.1. Double Decoupled Atomic Norm Minimization

First, we explore the sparsity of the covariance and pseudo-covariance matrices with the decoupled ANM (D-ANM) technique. The covariance matrix $\boldsymbol{R}_x$ in (5) can be rewritten as

$$\begin{aligned}\boldsymbol{R}_x &= \boldsymbol{A}\boldsymbol{R}_s\boldsymbol{A}^H = \boldsymbol{A}_{[K]}^K \text{diag}(\text{vec}(\boldsymbol{R}_s^T))(\boldsymbol{A}^K)^H \\ &= \sum_{i=1}^{K}\sum_{j=1}^{K} r_{i,j}\boldsymbol{a}(f_i)\boldsymbol{a}^H(f_j) = \sum_{l=1}^{K^2}\alpha_l \boldsymbol{a}(f_{1,l})\boldsymbol{a}^H(f_{2,l}) \\ &= \sum_{l'=1}^{K'}\gamma_{l'}\boldsymbol{a}(f_{1,l'})\boldsymbol{a}^H(f_{2,l'}) = \boldsymbol{A}(\boldsymbol{f}_1)\boldsymbol{\Gamma}\boldsymbol{A}^H(\boldsymbol{f}_2),\end{aligned} \tag{15}$$

where $\boldsymbol{A}_{[K]}^K = [\boldsymbol{A}_1^K, \dots, \boldsymbol{A}_K^K]$ with $\boldsymbol{A}_i^K = [\boldsymbol{a}(f_i), \dots, \boldsymbol{a}(f_i)] \in \mathbb{C}^{M\times K}$ and $\boldsymbol{A}^K = [\boldsymbol{A}, \dots, \boldsymbol{A}] \in \mathbb{C}^{M\times K^2}$. $\alpha_l = r_{i,j}$, $f_{1,l} = f_i$ and $f_{2,l} = f_j$ with $l = K(i-1)+j$. Note that α_l can be equal to zero according to (7). Accordingly, $\gamma_{l'}$ denotes the l'-th nonzero element in $\{\alpha_l\}_l$ and $f_{1,l'}$ as well as $f_{2,l'}$ is the corresponding frequency. K' is the number of nonzero elements in $\{\alpha_l\}_l$. Further, $\boldsymbol{A}(\boldsymbol{f}_1) = [\boldsymbol{a}(f_{1,1}), \dots, \boldsymbol{a}(f_{1,K'})]$, and $\boldsymbol{A}(\boldsymbol{f}_2) = [\boldsymbol{a}(f_{2,1}), \dots, \boldsymbol{a}(f_{2,K'})]$ with $\boldsymbol{f}_1 = [f_{1,1}, \dots, f_{1,K'}]^T$ and $\boldsymbol{f}_2 = [f_{2,1}, \dots, f_{2,K'}]^T$, respectively. Hence, $K' = |\{\boldsymbol{f}^{l'}\}_{l'}|$ with $\boldsymbol{f}^{l'} = (f_{1,l'}, f_{2,l'})$ is the number of frequency pairs constructing $\boldsymbol{R}_x$, or equivalently, the virtual source number of $\boldsymbol{R}_x$ from the view of two dimensional harmonic retrieval [13]. $\boldsymbol{\Gamma} = \text{diag}([\gamma_1, \dots, \gamma_{K'}]^T)$. Moreover, the pseudo-covariance matrix $\boldsymbol{C}_x$ in (6) can be rewritten as

$$\begin{aligned}\boldsymbol{C}_x &= \boldsymbol{A}\boldsymbol{C}_s\boldsymbol{A}^T = \boldsymbol{A}_{[K]}^K \text{diag}(\text{vec}(\boldsymbol{C}_s^T))(\boldsymbol{A}^K)^T \\ &= \sum_{i=1}^{K}\sum_{j=1}^{K} c_{i,j}\boldsymbol{a}(f_i)\boldsymbol{a}^T(f_j) = \sum_{l=1}^{K^2}\beta_l \boldsymbol{a}(f_{1,l})\boldsymbol{a}^H(-f_{2,l}) \\ &= \sum_{l'=1}^{K'}\eta_{l'}\boldsymbol{a}(f_{1,l'})\boldsymbol{a}^H(-f_{2,l'}) = \boldsymbol{A}(\boldsymbol{f}_1)\boldsymbol{\Sigma}\boldsymbol{A}^H(-\boldsymbol{f}_2),\end{aligned} \tag{16}$$

where $\beta_l = c_{i,j}$ with $l = K(i-1)+j$ and $\eta_{l'}$ denotes the l'-th nonzero element in $\{\beta_l\}_l$. Note that the indexes of nonzero elements in $\{\alpha_l\}_l$ and $\{\beta_l\}_l$ are the same according to (8) and $\alpha_l = r_{i,j}, \beta_l = c_{i,j}$ with $l = K(i-1)+j$, which implies the fifth and sixth equality in (16). $\boldsymbol{\Sigma} = \text{diag}([\eta_1, \dots, \eta_{K'}]^T)$ and $\boldsymbol{A}(-\boldsymbol{f}_2) = [\boldsymbol{a}(-f_{2,1}), \dots, \boldsymbol{a}(-f_{2,K'})]$.

Accordingly, it is easy to find that both $\boldsymbol{R}_x$ and $\boldsymbol{C}_x$ have a sparse linear atomic representation over the following matrix-form atom set

$$\mathcal{A}_d = \left\{\boldsymbol{a}(f_1)\boldsymbol{a}^H(f_2)\,|f_1, f_2 \in (-0.5, 0.5]\right\}. \tag{17}$$

Then, the atomic norms of both $\boldsymbol{R}_x$ and $\boldsymbol{C}_x$ can be defined to seek the sparsest decomposition of $\boldsymbol{R}_x$ and $\boldsymbol{C}_x$ over the atom set $\mathcal{A}_d$. In this sense, the D-ANM technique [14] can be used to jointly exploit the sparsity of both $\boldsymbol{R}_x$ and $\boldsymbol{C}_x$. Hence, with obtained $\hat{\boldsymbol{E}}_y$, we produce the following D-ANM formulation for NC coherent scenarios:

$$\min_{\boldsymbol{R}_x, \boldsymbol{C}_x} \tau_3' \left(\|\boldsymbol{R}_x\|_{\mathcal{A}_d} + \|\boldsymbol{C}_x\|_{\mathcal{A}_d}\right) + \frac{1}{2}\left\|\hat{\boldsymbol{E}}_y - \boldsymbol{J}\boldsymbol{R}_E\right\|_F^2, \tag{18}$$

where $\boldsymbol{R}_E = \left[\boldsymbol{R}_x\boldsymbol{J}^H, \boldsymbol{C}_x\boldsymbol{J}^T\right]$ and τ_3' is similarly defined as τ_1. Moreover, (18) is equivalent to the following SDP formulation [14]

$$\begin{aligned}\min_{\substack{\boldsymbol{R}_x, \boldsymbol{C}_x\\ \text{T}(\boldsymbol{u}_1), \text{T}(\boldsymbol{u}_2)}} \quad & \frac{\tau_3'}{M}\left(\text{Tr}(\text{T}(\boldsymbol{u}_1)) + \text{Tr}(\text{T}(\boldsymbol{u}_2))\right) + \frac{1}{2}\left\|\hat{\boldsymbol{E}}_y - \boldsymbol{J}\boldsymbol{R}_E\right\|_F^2 \\ \text{s.t.} \quad & \begin{bmatrix} \text{T}(\boldsymbol{u}_1) & \boldsymbol{R}_x \\ \boldsymbol{R}_x^H & \text{T}(\boldsymbol{u}_1)\end{bmatrix} \succeq 0, \begin{bmatrix} \text{T}(\boldsymbol{u}_2) & \boldsymbol{C}_x \\ \boldsymbol{C}_x^H & \text{T}^*(\boldsymbol{u}_2)\end{bmatrix} \succeq 0,\end{aligned} \tag{19}$$

where we enforce the Toeplitz matrices in the equivalent PSD constraint of $\|\boldsymbol{R}_x\|_{\mathcal{A}}$ to be the same and the counterparts in that of $\|\boldsymbol{C}_x\|_{\mathcal{A}}$ to be the conjugated. This is because the sets of distinct frequencies in $\boldsymbol{f}_1$ and $\boldsymbol{f}_2$ are the same and is $\{f_i\}_i$, which contains all the interested harmonic information. Hence, once either the Toeplitz matrices is obtained, we can retrieve the frequencies $\{f_i\}_i$ via Vandermonde decomposition techniques.

Subsequently, we present two mutual coupling characteristics between the covariance and pseudo-covariance matrices. First, based on the decomposition of $\boldsymbol{R}_x$ and $\boldsymbol{C}_x$ in (15) and (16) and the D-ANM theorem [14], the ideal optimal solutions of (19) as $\text{T}(\boldsymbol{u}_1)$ and $\text{T}(\boldsymbol{u}_2)$ can be expressed as

$$\begin{aligned}\text{T}(\boldsymbol{u}_1) &= \sum_{l'=1}^{K'}|\gamma_{l'}|\boldsymbol{a}(f_{1,l'})\boldsymbol{a}^H(f_{1,l'}) = \sum_{i=1}^{K}\left(\sum_{j=1}^{K}|r_{i,j}|\right)\boldsymbol{a}(f_i)\boldsymbol{a}^H(f_i) \\ \text{T}(\boldsymbol{u}_2) &= \sum_{l'=1}^{K'}|\eta_{l'}|\boldsymbol{a}(f_{1,l'})\boldsymbol{a}^H(f_{1,l'}) = \sum_{i=1}^{K}\left(\sum_{j=1}^{K}|c_{i,j}|\right)\boldsymbol{a}(f_i)\boldsymbol{a}^H(f_i).\end{aligned} \tag{20}$$

Accordingly, based on the unique Vandermonde decomposition lemma of Toeplitz matrices [15] and the equality in (9), we have $\text{T}(\boldsymbol{u}_1) = \text{T}(\boldsymbol{u}_2)$ in (19) when $K \le M-1$, which means the coupling characteristic between $\boldsymbol{R}_x$ and $\boldsymbol{C}_x$ can be enforced as $\text{T}(\boldsymbol{u}) = \text{T}(\boldsymbol{u}_1) = \text{T}(\boldsymbol{u}_2)$ in (19).

Moreover, the compressed augmented covariance matrix $\boldsymbol{R}_z$ of $\boldsymbol{z}(t) = [\boldsymbol{y}^T(t), \boldsymbol{y}^H(t)]^T$ can be expressed as [10]

$$\boldsymbol{R}_z = \mathbb{E}\{\boldsymbol{z}(t)\,\boldsymbol{z}^H(t)\} = \begin{bmatrix} \boldsymbol{R}_y & \boldsymbol{C}_y \\ \boldsymbol{C}_y^* & \boldsymbol{R}_y^*\end{bmatrix} = \boldsymbol{J}'\boldsymbol{R}_a\boldsymbol{J}'^H + \boldsymbol{R}_{n'}, \tag{21}$$

where

$$\boldsymbol{R}_a = \mathbb{E}\{\boldsymbol{x}_a(t)\,\boldsymbol{x}_a^H(t)\} = \begin{bmatrix} \boldsymbol{R}_x & \boldsymbol{C}_x \\ \boldsymbol{C}_x^* & \boldsymbol{R}_x^*\end{bmatrix} \tag{22}$$

denotes the augmented covariance matrix of $\boldsymbol{x}_a(t)$ and $\boldsymbol{R}_{n'}$ is the covariance of $\boldsymbol{n}'(t)$ with $\boldsymbol{n}'(t) = [\boldsymbol{n}^T(t), \boldsymbol{n}^H(t)]^T$, $\boldsymbol{x}_a(t) = [\boldsymbol{x}^T(t), \boldsymbol{x}^H(t)]^T$ and $\boldsymbol{J}' = \text{blkdiag}([\boldsymbol{J}, \boldsymbol{J}^*])$, respectively. Note that with known $\boldsymbol{J}'$, both $\boldsymbol{R}_z$ and $\boldsymbol{R}_a$ are constructed by $\boldsymbol{R}_x$ and $\boldsymbol{C}_x$ and they are both covariance matrix, which means $\boldsymbol{R}_z$ and $\boldsymbol{R}_a$ are both PSD matrices, i.e., $\boldsymbol{R}_z \succeq 0$ and $\boldsymbol{R}_a \succeq 0$. Moreover, note that $\boldsymbol{R}_z \succeq 0$ is implicit in $\boldsymbol{R}_a \succeq 0$ based on the properties of PSD matrices [16]. Hence, the other one manual coupling characteristic between $\boldsymbol{R}_x$ and $\boldsymbol{C}_x$ can be materialized as $\boldsymbol{R}_a \succeq 0$.

Consequently, by letting $\text{T}(\boldsymbol{u}_1) = \text{T}(\boldsymbol{u}_2) = \text{T}(\boldsymbol{u})$ and imposing $\boldsymbol{R}_a \succeq 0$ into (19), we have the proposed double D-ANM (DD-ANM)

$$\begin{aligned}&\{\widetilde{\boldsymbol{R}}_x, \widetilde{\boldsymbol{C}}_x, \text{T}(\widetilde{\boldsymbol{u}})\} \\ &= \arg\min_{\boldsymbol{R}_x, \boldsymbol{C}_x, \boldsymbol{T}} \frac{\tau_3}{M}\text{Tr}(\text{T}(\boldsymbol{u})) + \frac{1}{2}\left\|\hat{\boldsymbol{R}}_z - \boldsymbol{J}'\boldsymbol{R}_a\boldsymbol{J}'^H\right\|_F^2 \\ &\qquad \text{s.t.} \quad \begin{bmatrix} \text{T}(\boldsymbol{u}) & \boldsymbol{R}_x \\ \boldsymbol{R}_x^H & \text{T}(\boldsymbol{u})\end{bmatrix} \succeq 0\ , \quad \begin{bmatrix} \text{T}(\boldsymbol{u}) & \boldsymbol{C}_x \\ \boldsymbol{C}_x^H & \text{T}^*(\boldsymbol{u})\end{bmatrix} \succeq 0 \\ &\qquad\qquad \boldsymbol{R}_a \succeq 0\ , \quad \boldsymbol{R}_a \text{ in (22)},\end{aligned} \tag{23}$$

where $\tau_3 = 4\tau_3'$ since $\left\|\hat{\boldsymbol{R}}_z - \boldsymbol{J}'\boldsymbol{R}_a\boldsymbol{J}'^H\right\|_F^2 = 2\left\|\hat{\boldsymbol{E}}_y - \boldsymbol{J}\boldsymbol{R}_E\right\|_F^2$.

3.2. Harmonic Retrieval

By solving the proposed DD-ANM in (23), we can not only obtain the estimates of $\widetilde{\boldsymbol{R}}_x$ and $\widetilde{\boldsymbol{C}}_x$, but a PSD structured Toeplitz matrix

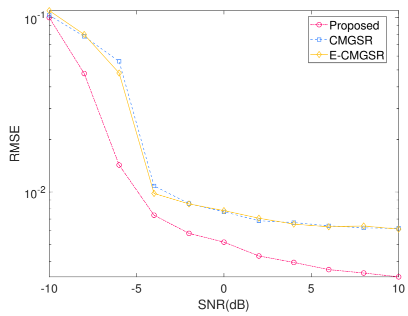

Fig. 1. RMSE versus SNR for the proposed TD-ANM, CMGSR and E-CMGSR with M=7, N=4, K=3, L=400 and M_t=300.

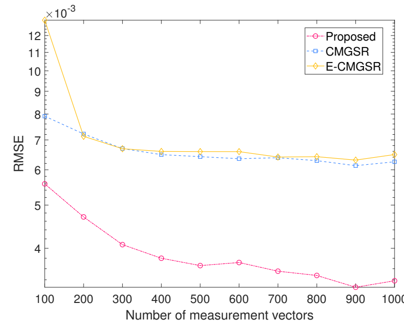

Fig. 2. RMSE versus number of measurement vectors L for the proposed TD-ANM, CMGSR and E-CMGSR with M=7, N=4, K=3, SNR=4dB and M_t=300.

$\mathrm{T}(\widetilde{\boldsymbol{u}})$, which is constructed by the interested frequencies as [17]

$$\mathrm{T}(\widetilde{\boldsymbol{u}}) = \sum_{i=1}^{K} \mu_i \boldsymbol{a}(\widetilde{f}_i)\boldsymbol{a}^H(\widetilde{f}_i) = \sum_{i=1}^{K}\left(\sum_{j=1}^{K} |\widetilde{r}'_{i,j}|\right)\boldsymbol{a}(\widetilde{f}_i)\boldsymbol{a}^H(\widetilde{f}_i), \tag{24}$$

where $\widetilde{f}_i$ is the estimate of f_i and $\mu_i = \sum_{j=1}^{K} |\widetilde{r}'_{i,j}|$. Given $\mathrm{T}(\widetilde{\boldsymbol{u}})$ in (24), the Vandermonde decomposition techniques can be applied for harmonic retrieval, such as, the MUSIC [18] and ESPRIT [19].

3.3. Theoretical Analysis

In this subsection, we give a brief discussion on the fundamental limits of the proposed DD-ANM method, which is derived by using the results from our recent work in [13]. To this end, we consider the following sub-optimization programming of the proposed method :

$$\min_{\boldsymbol{R}_x} \|\boldsymbol{R}_x\|_{\mathcal{A}_d} \quad \text{s.t.} \quad \mathrm{vec}(\hat{\boldsymbol{R}}_y) = \boldsymbol{\Psi}\mathrm{vec}(\boldsymbol{R}_x), \tag{25}$$

where $\boldsymbol{\Psi} = \boldsymbol{J}^* \otimes \boldsymbol{J}$ in the proposed case. Then, for a generalized $\boldsymbol{\Psi} \in \mathbb{C}^{N' \times M^2}$, according to Theorem 1 in [13], we have the following fundamental limits.

Theorem 1: Let $\boldsymbol{\Psi}$ be a random matrix with rows $\boldsymbol{\psi}_i^H$ chosen independently from a distribution obeying the isotropy and incoherence properties [20] with some fixed $\zeta \geq 1$. Assume that the phase terms ϕ_i in $\boldsymbol{s}(t)$ is symmetrically distributed around 0 between $\left[-\frac{\pi}{2}, \frac{\pi}{2}\right]$ and all the frequencies obey the minimum separation condition

$$\min_{i \neq j} |f_i - f_j| \geq \frac{5}{N}. \tag{26}$$

Then, the programming in (25) returns the true $\boldsymbol{R}_x$ as well as the frequencies $\{f_i\}_i$ with a probability at least $1-\delta$, as long as

$$N' \geq C\zeta K' \log^2(M/\delta), \tag{27}$$

with C being a constant.

Although the bound in Theorem 1 is too tough for the proposed DD-ANM since it only considers one D-ANM in the proposed method, it offers a guide to the relationship between the measurement vector length N' and the virtual source number K'. That is N', aka the allowable compression, is lower bounded by a function of K', which is determined jointly by the source number K and the coherency among the source signals.

4. NUMERICAL SIMULATIONS

This section presents numerical results to evaluate the performance of the proposed DD-ANM solution. The CMGSR [9] and the E-CMGSR are simulated as benchmarks. All the methods are implemented with the regularization parameter $\tau_i = 1$ $(i = 1, 2, 3)$ and employed with conventional Root-MUSIC algorithm [21] for frequency retrieval. The root mean squared error (RMSE) is used to measure the estimation accuracy of harmonic retrieval as RMSE $= \frac{1}{K}\sum_{k=1}^{K}\left(\frac{1}{M_t}\sum_{n=1}^{M_t}(\widetilde{f}_k^n - f_k)^2\right)^{\frac{1}{2}}$, where M_t and $\widetilde{f}_k^n$ are the number of Monte-Carlo trials and the estimates of f_k in the n-th trial.

We consider $\boldsymbol{J} = \boldsymbol{I}_\Omega$ with selection indices $\Omega = \{1, 2, 5, 7\}$ and there are three equal-power source signals with $\boldsymbol{f} = [-0.3, 0, 0.2]$ and $\boldsymbol{\phi}$ being selected uniformly from $(0, \pi]$. For coherent scenarios, we consider the first and second source signals are coherent while the third source signal is uncorrelated with them. We compare the RMSE of different algorithms versus the SNR with $L = 400$. Fig. 1 indicates that the E-CMGSR method cannot achieve desired performance improvement compared with the CMGSR algorithm. This is because the number of measurements is larger than that of source signals, i.e., $K < N$, and $N = 4$ is relative small, which leads to doubling the number of measurements ($N' = 8$) makes a rare contribution to the performance improvement. In contract, the proposed DD-ANM achieves the best performance among these methods due to it captures the sparsity of the interested common frequencies of the covariance and pseudo-covariance matrices and permits the PSD characteristic of the estimate of the augmented matrix. Fig. 2 presents the RMSE performance of these approaches for different L, which reveals a similar trend as that shown in Fig. 1.

5. CONCLUSION

This paper proposes a super-resolution harmonic retrieval method for NC coherent signals. We first develop gridless sparse representations of both the covariance and pseudo-covariance matrices over a common matrix-form atom set, which permits the D-ANM technique to jointly exploit the sparsity of them. Then, by utilizing the inherent mutual coupling characteristics between them, we introduce additional constraints to properly reflect and enforce some desired structure information represented by such matrices and their augmented matrix, which finally give rise to the proposed DD-ANM for harmonic retrieval of NC coherent signals. Theoretical analysis and simulation results validate the merit of the DD-ANM method with higher estimation performance beyond existing benchmarks.

6. REFERENCES

[1] Frederic Barbaresco and Pascal Chevalier, "Noncircularity exploitation in signal processing overview and application to radar," in *2008 IET Waveform Diversity & Digital Radar Conference*, 2008, pp. 1–6.

[2] Yue Wang and Zhi Tian, "Big data in 5G," in *Encyclopedia of Wireless Networks*, pp. 96–106. Springer, 2020.

[3] Feifei Gao, Yide Wang, and A Nallanathan, "Improved MUSIC by exploiting both real and complex sources," in *2006 IEEE Military Communications conference (MILCOM)*. IEEE, 2006, pp. 1–6.

[4] Sonia Ben Hassen, Faouzi Bellili, Abdelaziz Samet, and Sofiène Affes, "DOA estimation of temporally and spatially correlated narrowband noncircular sources in spatially correlated white noise," *IEEE Transactions on Signal Processing*, vol. 59, no. 9, pp. 4108–4121, 2011.

[5] Xin-Yu Sun, Jian-Jiang Zhou, and Hua-Wei Chen, "Low complexity direction-of-arrival estimation of coherent noncircular sources," *Multidimensional Systems and Signal Processing*, vol. 27, pp. 159–177, 2016.

[6] Yuexian Wang, Matthew Trinkle, and Brian W-H Ng, "Efficient DOA estimation of noncircular signals in the presence of multipath propagation," *Signal Processing*, vol. 149, pp. 14–26, 2018.

[7] Weijie Tan, Xian Feng, Xinrong Ye, and Lianyou Jing, "Direction-of-arrival of strictly non-circular sources based on weighted mixed-norm minimization," *EURASIP Journal on Wireless Communications and Networking*, vol. 2018, no. 1, pp. 1–10, 2018.

[8] Jiao Zhang, Xiangyu Ren, Jianan Li, Yufeng Liu, and Wenmei Zhang, "DOA estimation of non-circular signals based on iterative soft thresholding algorithm," *International Journal of RF and Microwave Computer-Aided Engineering*, vol. 32, no. 11, pp. e23391, 2022.

[9] Xue Zhang, Zhi Zheng, Wen-Qin Wang, and Hing Cheung So, "DOA estimation of coherent sources using coprime array via atomic norm minimization," *IEEE Signal Processing Letters*, vol. 29, pp. 1312–1316, 2022.

[10] Yu Zhang, Yue Wang, Zhi Tian, Geert Leus, and Gong Zhang, "Super-resolution harmonic retrieval of non-circular signals," in *2023 IEEE International Conference on Acoustics, Speech and Signal Processing (ICASSP)*. IEEE, 2023, pp. 1–5.

[11] Yuanxin Li and Yuejie Chi, "Off-the-grid line spectrum denoising and estimation with multiple measurement vectors," *IEEE Transactions on Signal Processing*, vol. 64, no. 5, pp. 1257–1269, Mar. 2016.

[12] Michael Grant and Stephen Boyd, "CVX: Matlab software for disciplined convex programming, version 2.1," `http://cvxr.com/cvx`, Mar. 2014.

[13] Yu Zhang, Yue Wang, Zhi Tian, Geert Leus, and Gong Zhang, "Efficient super-resolution two-dimensional harmonic retrieval with multiple measurement vectors," *IEEE Transactions on Signal Processing*, vol. 70, pp. 1224–1240, 2022.

[14] Zhe Zhang, Yue Wang, and Zhi Tian, "Efficient two-dimensional line spectrum estimation based on decoupled atomic norm minimization," *Signal Processing*, vol. 163, pp. 95–106, 2019.

[15] Zai Yang and Lihua Xie, "On gridless sparse methods for line spectral estimation from complete and incomplete data," *IEEE Transactions on Signal Processing*, vol. 63, no. 12, pp. 3139–3153, 2015.

[16] Xian-Da Zhang, *Matrix analysis and applications*, Cambridge University Press, 2017.

[17] Yue Wang, Yu Zhang, Zhi Tian, Geert Leus, and Gong Zhang, "Super-resolution channel estimation for arbitrary arrays in hybrid millimeter-wave massive MIMO systems," *IEEE Journal of Selected Topics in Signal Processing*, vol. 13, no. 5, pp. 947–960, Sept. 2019.

[18] Ralph Schmidt, "Multiple emitter location and signal parameter estimation," *IEEE Transactions on Antennas and Propagation*, vol. 34, no. 3, pp. 276–280, 1986.

[19] Richard Roy and Thomas Kailath, "ESPRIT-estimation of signal parameters via rotational invariance techniques," *IEEE Transactions on acoustics, speech, and signal processing*, vol. 37, no. 7, pp. 984–995, 1989.

[20] Reinhard Heckel and Mahdi Soltanolkotabi, "Generalized line spectral estimation via convex optimization," *IEEE Transactions on Information Theory*, vol. 64, no. 6, pp. 4001–4023, 2017.

[21] Arthur Barabell, "Improving the resolution performance of eigenstructure-based direction-finding algorithms," in *1983 IEEE International Conference on Acoustics, Speech, and Signal Processing (ICASSP)*. IEEE, 1983, vol. 8, pp. 336–339.